

UDC 622.24:622.276

NUMERICAL SIMULATION OF POLYCRYSTALLINE DIAMOND COMPACT BIT ROCK-BREAKING PROCESS BASED ON SMOOTH PARTICLE HYDRODYNAMIC-FINITE ELEMENT COUPLING METHOD

J.PeI, Z.Yinghu, W.Zhenquan, S.Dongyu,
(China University of Petroleum)

In order to study the dynamic response characteristic of the rock-breaking process by polycrystalline diamond compact (PDC) bit cutters, a three dimensional numerical model of rock-breaking is set up based on smooth particle hydrodynamic-finite element (SPH-FE) coupling method, and the influence factors are analyzed. Research shows:

- the spread of stress wave in rock has obvious local effect and the rock-breaking process has "leap form" characteristic;
- cutting force and axial force increase approximate linearly with the increasing of cutting depth;
- the increase of cutting speed will accelerate the process of rock-breaking, but has little effect on the cutting force;
- the cutting angle is closely related to rock-breaking efficiency, and the optimization of cutting angle depends upon lithology,
- the optimum cutting angle of shale, sandstone and granite should be between $3^{\circ}\sim 7^{\circ}\sim 4^{\circ}\sim 1^{\circ}$ and $1^{\circ}\sim 5^{\circ}$ respectively.

Keywords: polycrystalline diamond compact drill bit (PDC drill bit), smoothed particle hydrodynamics-finite element coupling method (SPH-FE) method, crack propagation, rock-breaking efficiency.

E-mail: jpnt2005@163.com

DOI: 10.5510/OGP20130300165

1. Introduction

Studying the mechanical behavior of PDC drill bit rock-breaking process is the basis of the optimal design of PDC bit cutting structure. Early scholars researched the coal petrography breaking process mainly based on the theory of metal cutting, and put forward the theories of tensile failure [1] and shear failure [2] of rock, but there exists many uncertainty factors in the rock-breaking process, theoretical studies tends to far cry from the practical rock-breaking condition. scholars carried out a large number of indoor test to simulate rock-breaking process [3-5], but owing to the comprehensive influence of rock properties and cutting structural parameters, it is bound to do a great deal of experiments to get the relationship between cutting structures and rock-breaking efficiency systematically.

In recent years, numerical simulation method has been applied to the research of rock-breaking because of its simple and efficient [6, 7], this method just needs to adjust model, material and loading style through computer, not only can eliminate the influence of boundary effect which the experiment is inevitable, but also can carry out repeated experiments of complex conditions flexibly and easily once the simulation results are verified by the hardware experiments, which can save a lot of human, physical and financial resources.

Usually scholars use finite element or finite difference method to analyze rock-breaking process, these methods are based on continuum mechanics, have strong dependence on the mesh, and are not good at dealing with discontinuity problems which mesh deformation serious [8, 9]. However, rock-breaking process is a development process from continuous to discontinuous, the movement of particles after cracking

is discontinuous and complicated, so it surly exists flaw in calculation precision.

Smooth particle hydrodynamic method (SPH) can simulate the constitutive behavior of complex materials without using the mesh, it can well solve the problem of large deformation and crack extension which traditional numerical simulation methods can't solve very well [10]. But due to the complex meshless interpolation calculation, the computation is huge generally, while the finite element method has higher computational efficiency than the SPH method when calculating continuum deformation problem.

Coupling SPH-FE method is adopted to simulate rock-breaking process, the advantages of both SPH and FE method are exerted fully. Also the simulation results are verified by hardware experiment, and finally the optimal cutting structure parameters of different rock is proposed.

2. Contact Algorithm of Coupling SPH-FE Method

The coupling SPH-FE method was proposed by Attaway and Johnson [11, 12], and was widely used in the analysis of large deformation of fluid and ballistic impact, crack propagation problems [13, 14]. The contact algorithm between the SPH particles and FE nodes is the key problem of coupling SPH-FE method, early scholars analyzed this contact algorithm mainly based on master-slave structure algorithm [15], this algorithm needs to build the contact surface and calculate the normal of the surface, which need too much computation. Particle-particle contact algorithm is used in this paper, there could have non-friction sliding between SPH particles and FE elements, the contact force is exerted according to particle smooth length which does not need to define the contact particle, and

the contact force vector is calculated by treating FE nodes as SPH particles, also the magnitude of contact force applied upon SPH particles is determined by the resultant force of all FE nodes in search field, and do not need to define contact surface and surface normal, which is very suitable for the analysis of various forms of collision contact problems and FE mesh deformation serious conditions.

Defining starting point of contact algorithm by contact potential function ϕ_c :

$$\phi_c(x_i) = \int_{\Omega} K \left(\frac{W(x_i - x)}{W(h_{avg})} \right)^n dV \quad (1)$$

K , n - parameters represent the size and shape of contact potential field;

h_{avg} - average smooth length between particles or nodes;

h - smooth length of SPH particle;

W - kernel function used for SPH interpolation algorithm, the commonly used kernel function at

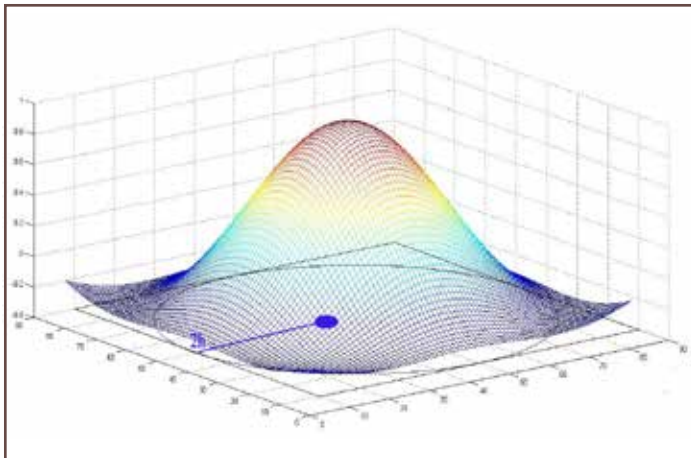


Fig.1. Cubic spline kernel function diagram

present is cubic spline function (shown in fig.1); $2h$: search radius of center SPH particle.

The contact sketch between SPH particles and FE nodes is shown in figure 2, the red points represent SPH particles, the gray points represent FE nodes, the circle of radius $2h$ represents search domains of SPH particle x_i . The FE nodes are regarded as SPH particles in the search domains, and the interaction force between SPH particles and FE nodes is calculated by particle-particle contact algorithm.

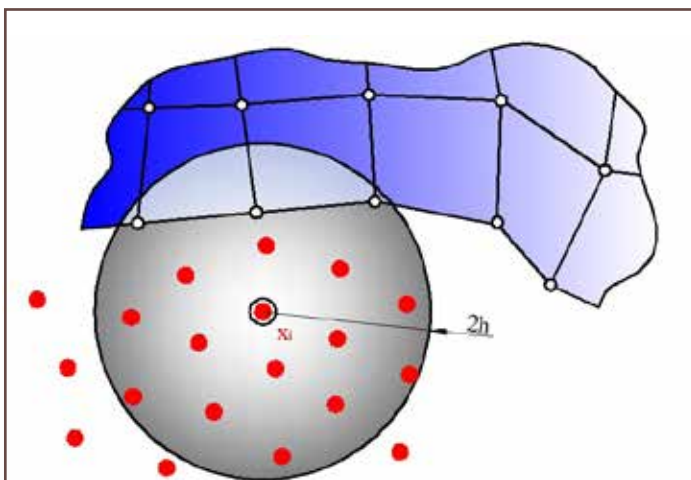


Fig.2. Contact sketch of SPH particles and FE nodes

The body force $b(x_i)$ of SPH particle x_i is the sum of component force of SPH particles and FE nodes in the search domains.

$$b_c(x_i) = \nabla \phi(x_i) = \sum_j^N \frac{m_j}{\rho_j} K n \frac{W(x_i - x_j)^{n-1}}{W(h_{avg})^n} \nabla_{x_i} W(x_i - x_j) \quad (2)$$

Where: m_j - the mass of particle/node j ;

ρ_j - the density of particle/node j ;

N - the number of particles/nodes in the search domains of x_i .

The contact force vector can be expressed as:

$$f_c(x_i) = \sum_j^N \frac{m_j}{\rho_j} \frac{m_i}{\rho_i} K n \frac{W(x_i - x_j)^{n-1}}{W(h_{avg})^n} \nabla_{x_i} W(x_i - x_j) \quad (3)$$

The FE nodes are regarded as SPH particles in formula 3, and the smooth length is determined according to adjacent element size.

3. Numerical Simulation of Rock-Breaking Process by Single Cutter

This paper analyzes rock-breaking process using coupling SPH-FE method which based on LS-DYNA program. The meshless particles are used to simulate the large deformation, broken and sprinkling of rock in the area that finite element mesh would occur serious distortion to ensure computational accuracy; the finite element mesh are used in the circumjacent area that the mesh is protected good to ensure computational efficiency, which giving full play to the advantage of both SPH particles and FE elements.

3.1. Material model and damage criterion of rock

The plastic kinematic hardening model which considering strain rate and damage effect is used to calculate rock-breaking behavior under large deformation, isotropic or kinematic hardening, the influence of temperature on the material is not taken into account.

Because the change of strain (especially plastic strain which used as internal variable) can reflect the loading path, loading history and the entire failure process of rock-breaking [16], the plastic strain is adopted as the criterion of rock damage. When the equivalent plastic strain of rock reaches to the value that rock is failure completely, rock is damaged and stripping from the body.

Figure 3 shows the stress-strain curve of sandstone

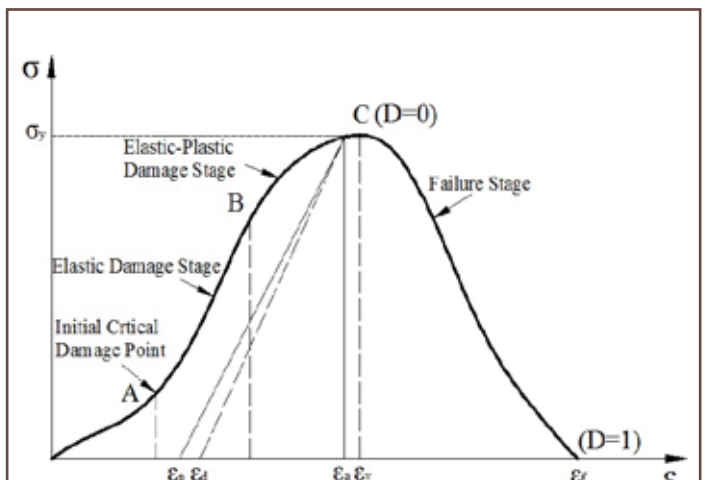


Fig.3. Stress-strain curve of sandstone somewhere

Material parameters of rocks and cutter

Table 1

	Density, kg/m ³	Elastic modulus, pa	Tangent modulus, pa	Yield strength, pa	Poisson ratio
Granite	2640	5E10	0.5E10	6E7	0.28
Shale	2640	2E10	0.2E10	1.5E7	0.15
Sandstone	2650	3.7E10	0.4E10	4.5E7	0.25
Polycrystalline diamond	2790	8E11			0.07
Tungsten carbide	7850	7E11			0.21

somewhere. ϵ_d and ϵ_p are the equivalent plastic strain at any point which does not consider and considers damage accumulation and evolution in the process of plastic damage mechanism transformation respectively, ϵ_f is the equivalent plastic strain when rock fails completely, ϵ_y and σ_y is the equivalent strain and stress respectively when rock begins to yield. D is the damage factor, when rock begins to break, $D = 0$; when rock fails and flakes off completely, $D = 1$.

All parameters of rock and cutter are given in table 1.

3.2 Numerical simulation model

PDC drill bit penetrates into the formation under the coaction of pressure and rotate speed, the movement of cutters can be seen as a helix progress process. The penetration depth is generally 2-6 mm when the cutters rotate a circle, which is far less than the diameter of drill bit, and the helix angle is small, so the helical motion of cutters can be simplified as plane movement, and velocity of 0.1 m/s in the X direction is loaded on the cutter. In the simulation, the size of rock is 60×60×40 mm, all the degrees of freedom of the rock boundary are constrained, the nonreflecting boundary conditions are loaded on both surrounding and bottom surfaces of the rock in order to avoid the effect of the boundaries wave reflection and simulate the infinite rock, the SPH particles are adopted to discrete the center of the rock. The front of the cutter is polycrystalline diamond thin layer and the rear of the cutter is tungsten carbide substrate, the polycrystalline diamond thin layer and tungsten carbide substrate are connected in the form of "glue", and the scarf joint way is ignored, keeping the elevation angle of the cutter 0° unchanged, the 3D model of rock-breaking is shown in figure 4.

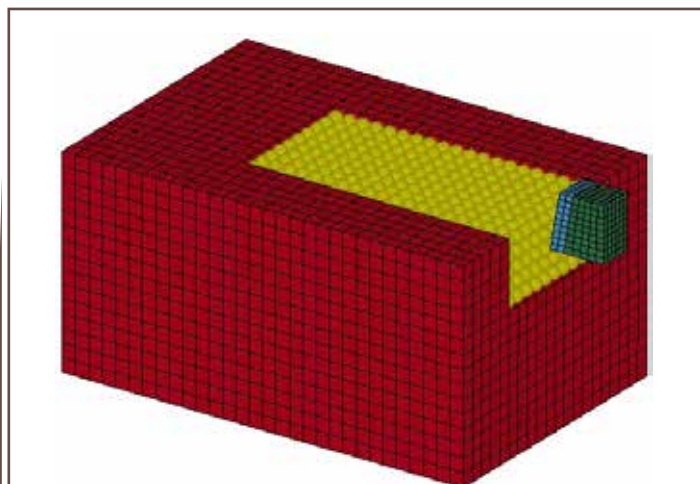


Fig.4. 3D model of rock-breaking

4. Results and Discussion

Because there are large number of calculated results and curves, and the trend of relationship between cutting depth, cutting deep and resultant cutting force is similar for different kind of rocks, granite is taken as an example to illustrate the results.

4.1 Dynamic response of rock-breaking process

The 3D-visualization of time-position-stress in different x-position is shown in figure 5, the cutting angle is -15°, cutting depth is 0.4cm and cutting speed is 0.5 m/s.

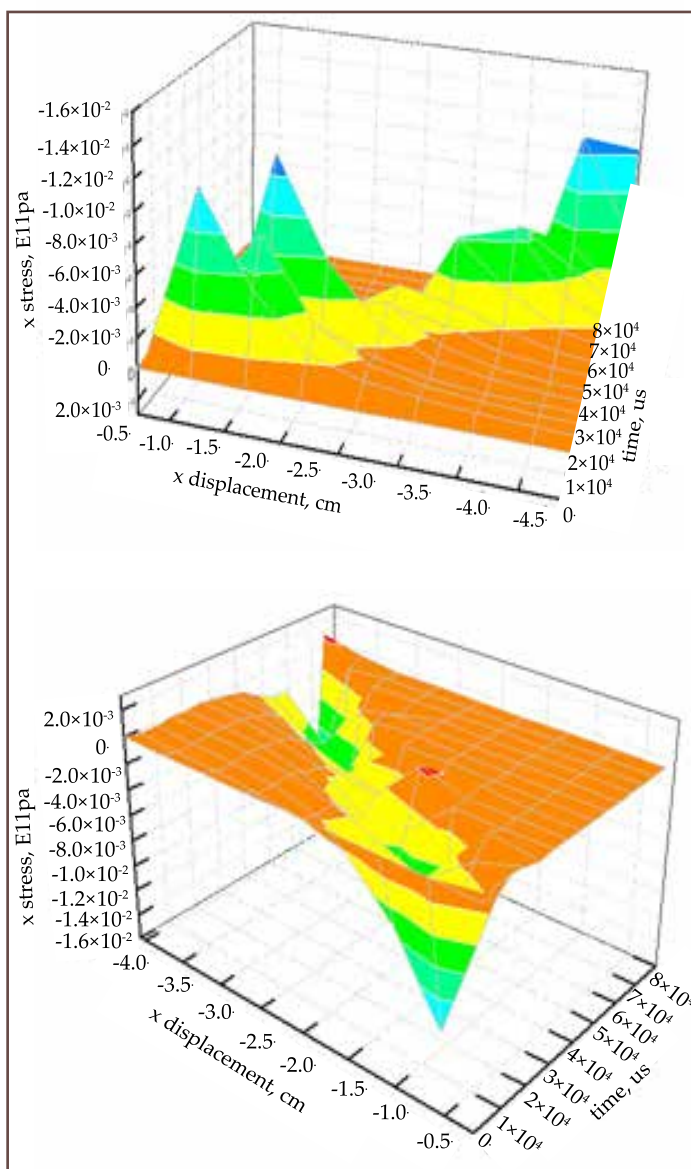


Fig.5. 3D-visualization of time-position-stress in different x-position of granite

For a particular rock unit, because the stress wave propagates in the rock, there would exist a small stress value when the cutter doesn't cut this unit; for the rock unit which is far away from the cutting area, it isn't subject to the force due to the great attenuation of stress wave energy, and this phenomenon shows that the stress wave has obvious local effect. When the cutter cuts a particular rock unit, the stress in this unit comes to peak, after a few times of stress fluctuation, this rock unit is damaged, with the cutter away from the rock unit, the stress in the unit decreases and finally tends to zero. This process reflects the dynamic response feature of rock (shown in fig.5). The cloud chart of Von Mises equivalent stress at different time for granite is shown in fig.6 (orthograph).

$t = 0.06$ s, Von Mises stress in the rock unit cut by cutter increases gradually, plastic deformation occurred in this unit (shown in (a));

$t = 0.105$ s, stress response area increases, stress value of the rock in front of cutter reaches or nears to damage value, damage factor D keeps increasing (shown in (b));

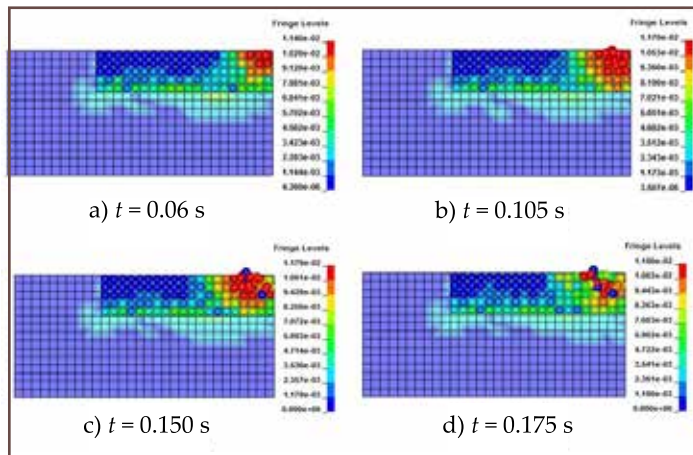


Fig.6. Von Mises equivalent stress at different time of granite

$t = 0.150$ s, the cuttings uplifts, local rock unit is damaged and $D = 1$ (shown in (c)). $t = 0.175$ s, rock unit avalanches, the cutter cuts in suddenly, and the cutting resistance descends instantaneously, cutter contacts with new rock element (shown in (d)). The cutter and rock experience a cycle process of contact-damage-contact again, which reflects "leap form" rock-breaking characteristics. Pont A represents the end and start of each leap process, where cuttings avalanches and resultant force drops suddenly (shown in fig.7).

4.2 Influence of cutting depth

The relationship between cutting force, axial force and cutting depth is shown in fig.8, the cutting angle is -15° and cutting speed is 0.3 m/s.

Through data fitting, cutting force and axial force increase linearly with the increasing of cutting depth, the increase range of axial force is relatively gradual than cutting force.

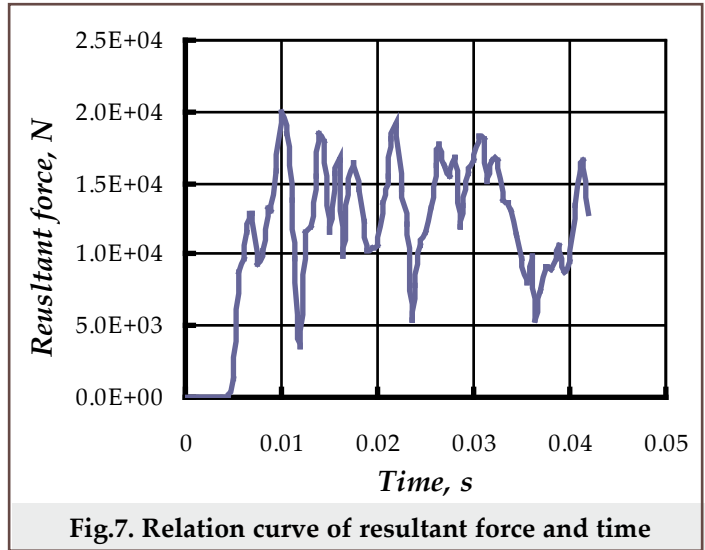


Fig.7. Relation curve of resultant force and time

4.3 Influence of cutting velocity

The relationship between cutting force, axial force and cutting speed is shown in fig.9, the cutting angle is -10° and cutting depth is 0.4 sm.

In general, cutting speed has very few effect on cutting force, and has no obvious impact on the propagation of crack and strength of rock, this agrees with the conclusions that given by C.Fairhurs [17]. But it is very clear that the increasing of cutting speed will accelerate the process of rock-breaking.

4.4 Influence of cutting angle

Cutting angle is closely related to rock-breaking efficiency. Taking negative cutting angle for example, the contact area between the cutter and rock unit increases with the increasing of cutting angle, and the compression stress of the rock unit decreases, which is easy to form a large volume of shear breakage, but there is also a problem that the polycrystalline diamond compact is easy to burst and damage. So there exists an optimal value of the cutting angle, and this value relates to the formation characteristics. Taking specific work (the work that required to break per unit volume of rock) as evaluation index, fig.10 shows the relation between cutting angle and specific work of shale, sandstone and granite respectively with cutting depth

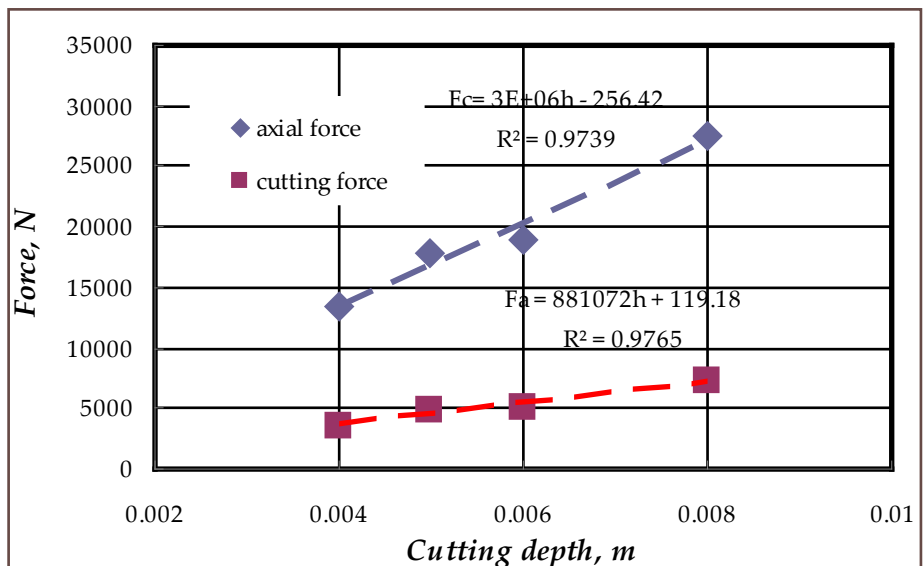


Fig.8. Relation curve of force and cutting depth

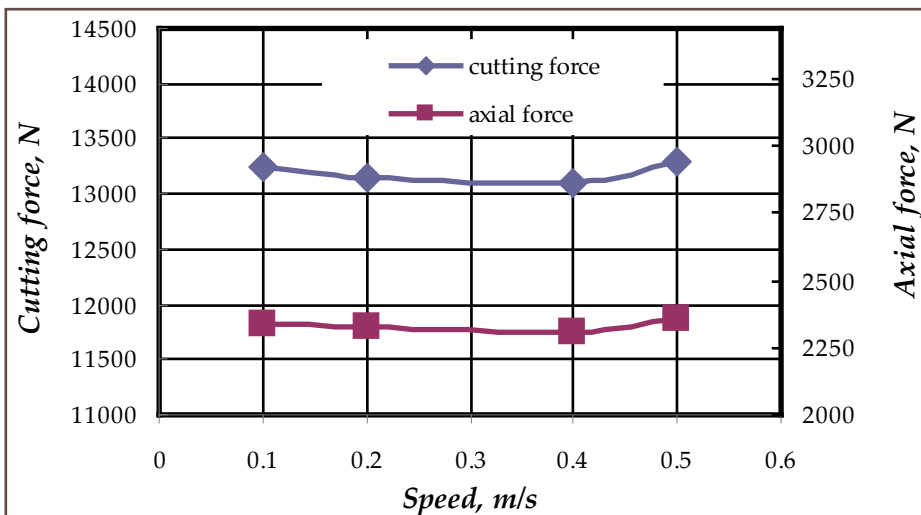


Fig.9. Relation curve of force and cutting speed

When cutting angle is positive, cutter breaks rock in the manner of shearing and stretching, the pressure that required to penetrate into the formation is smaller. So it suggests to choose positive and large cutting angle as far as possible.

5. Experimental Verification

Corresponding experimental study has been done to verify the correctness and reliability of simulation model. Experiments were carried out in the indoor rock-breaking bench testing machine (shown in fig.11), the diameter of PDC bit is 4-5/8" and the cutting angles are -15°~-10°~0°~5° and 10° respectively (shown in fig.12), rock

0.3cm and cutting speed 0.5m/s unchanged.

Because $K_{shale} < K_{sandstone} < K_{granite}$ (K- drillability), the specific work increases in turn for shale, sandstone and granite, the specific energy required to break granite is much higher than sandstone and shale, which shows that PDC drill bit is suitable for soft to medium hard formation in a certain extent. The optimal cutting angles of shale, sandstone and granite are between 3°~7°~4°~1° and 1°~5° respectively (shown in fig.10). When cutting angle is negative, cutter breaks rock in the manner of compress, and it is difficult to penetrate into the formation, the cutting efficiency is low especially for hard plastic formation.

core is granite, drilling depth is 50 mm, rotary speed is 40 rmp, delivery volume is 5 ml/min and weight of bit (WOB) are 3KN, 5KN and 8KN respectively.



Fig.11. Bench testing machine of rock-breaking

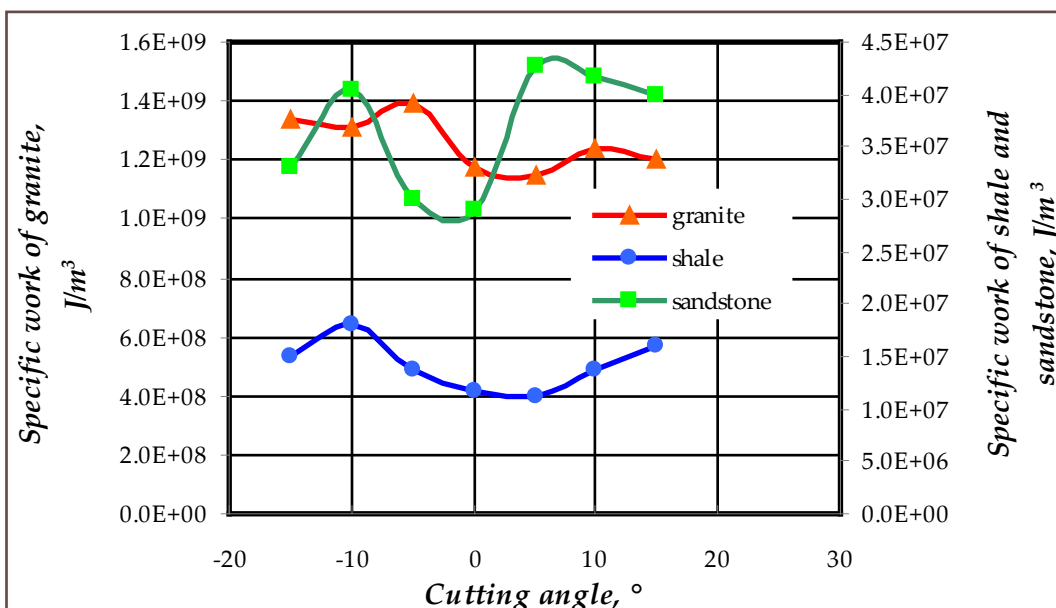


Fig.10. Relation curve of specific work and cutting angle

The change rule of specific work with cutting angle is similar for different pressure, the greater the pressure, the smaller the specific work, the optimal cutting angle is between 0°~5° (shown in fig.13), which is well coincident with the simulation result (shown in fig.10). Because the cutting angle of -5° is not adopted in the experiment, and there exists vibration of bench testing machine, there are some differences in the value of experiment and simulation result curve.

6. Conclusion

1. The results of simulation based on coupling SPH-FE method and experiment are in good consistence, the numerical simulation model could be used to instead experiment for the research of cutting structure.
2. The study of rock-breaking dynamic response shows that, the stress wave has obvious local effect, and the rock-breaking process has "leap form" characteristic.
3. Cutting force and axial force increase linearly with the increasing of cutting depth. The increasing of cutting speed will accelerate the process of rock breaking, but cutting speed has little effect on cutting force.
4. Cutting angle is closely related to rock-breaking efficiency and formation characteristics. The



Fig. 12. Experiment PDC bit with cutting angle 0°

optimal cutting angles of shale, sandstone and granite are between 3°~7°~4°~1° and 1°~5° respectively.

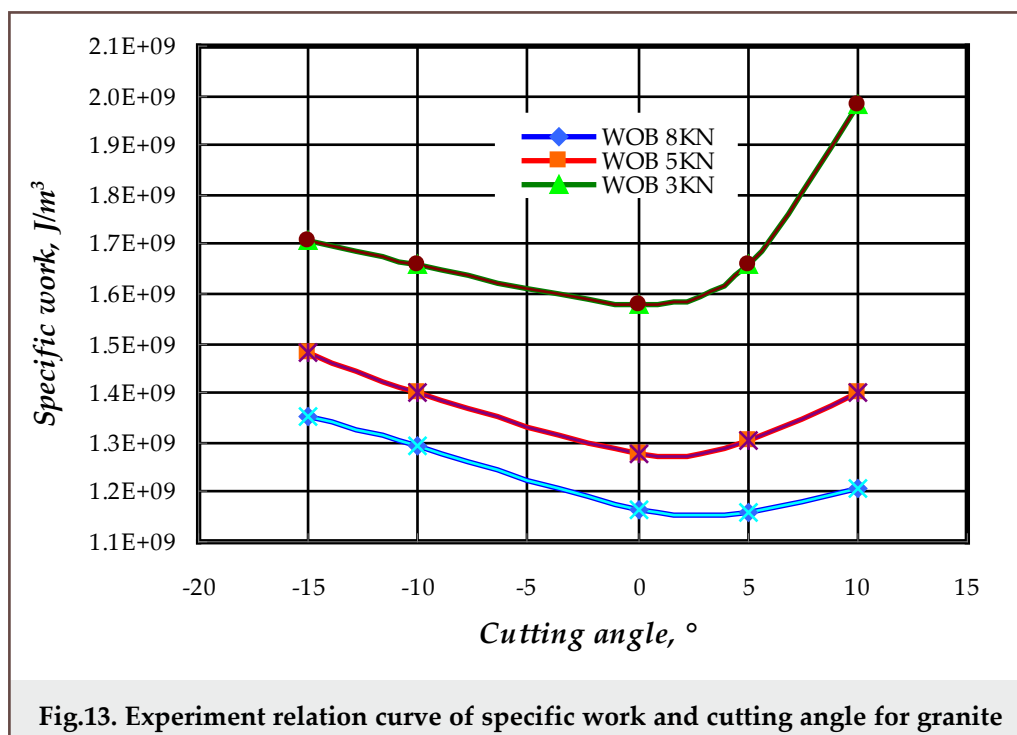


Fig.13. Experiment relation curve of specific work and cutting angle for granite

References

1. I.Evans. A theory of the basic mechanics of coal ploughing //Proc. Int. Symp. of Min. Res. -1962. -V. 2. -P.761-798.
2. Y.Nishimatsu. The mechanics of rock cutting //International Journal of Rock Mechanics and Mining Sciences & Geomechanics. -1972. -V.9. -No2. -P.261-270.
3. Z.Yinghu. Research of PDC bit design theory and method. Dissertation on competition of a engineering degree of Ph.D. Oil. China: China University of Petroleum. 1990.
4. L.Erguo, L.Zifeng, Z.Deyong. Experimental research on integrated mechanical model of PDC bit // Rock and Soil Mechanics. -2009. -V.30. -No4. -P.938-942.
5. Z.Deyong, C.Jifei, Y.un, etc. Optimization design of the cutter size and back rake for PDC bit in hard formation //Petroleum Drilling Techniques. -2011. -V.39. -No6. -P.91-94.
6. M.Qingming, W.Ruihe. Numerical simulation study on force of PDC cutter cutting rock //Drilling & Production Technology. -2006. -V.29. -No4. -P.78-80.
7. I.K.Gamwo, et al. Finite Element Modeling of Rock Cutting //44th US Rock Mechanics Symposium and 5th US-Canada Rock Mechanics Symposium. Salt Lake City. -2010.
8. K.Liu, S N.Melkote. Finite element analysis of the influence of tool edge radius on size effect in orthogonal micro-cutting process //International Journal of Mechanical Sciences. -2007. -V.49. -No5. -P.650-660.
9. K.C.Ee, O.W.Dillon, I.S.Jawahir. Finite element modeling of residual stresses in machining induced by cutting using a tool with finite edge radius //International Journal of Mechanical Sciences. -2005. -V.47. -No10. -P.1611-1628.

10. *J.Campbell, R.Vignjevic, L.Libersky*. A contact algorithm for smoothed particle hydrodynamics //Computer Methods in Applied Mechanics and Engineering. -2000. -V.184. -No1. -P.49-65.
11. *S.W.Attaway, M.W.Heinstein, J.W.Swegle*. Coupling of smooth particle hydrodynamics with the finite element method //Nuclear engineering and design. -1994. -V.150. -No2. -P.199-205.
12. *G.R.Johnson, S.R.Beissel*. Normalized smoothing functions for SPH impact computations //International Journal for Numerical Methods in Engineering. -1996. -V.39. -No16. -P.2725-2741.
13. *M.Sauer*. Simulation of high velocity impact in fluid-filled containers using finite elements with adaptive coupling to smoothed particle hydrodynamics //International Journal of Impact Engineering. -2011. -V.38. -No6. -P.511-520.
14. *Y.Chuzel-Marmot, R.Ortiz, A.Combescure*. Three dimensional SPH-FEM gluing for simulation of fast impacts on concrete slabs //Computers & Structures. -2011. -V.89. -No23. 2484-2494.
15. *M.Sauer*. Adaptive Kopplung des Netzfreen SPH-Verfahrensmit Finiten Elementen zur Berechnung von Impaktvorgängen, PhD thesis, Universit.at der Bundeswehr M.unchen (Deutschland), 2000.
16. *H.Gao, Y.Zheng, X.Feng*. Exploration on yield and failure of materials[J]. Chinese Journal of Rock Mechanics and Engineering, 2006, 25(12): 2.
17. *C.Fairhurst*. Some possibility and limitations of rotary drilling in hard rocks //Transaction of the instruction of mining engineers. -1956. -V.115. -P.85~103.

**Численное моделирование процесса разрушения породы
поликристаллическим алмазным компактным долотом,
основанное на объединенном методе гидродинамики
сглаженных частиц – конечных элементов**

Ж.Пеи, З.Йингху, В.Женгуан, С.Донгью
(Китайский Нефтяной Университет)

Реферат

С целью изучения основных динамических характеристик в процессе разрушения породы при бурении поликристаллическими алмазными компактными (ПАК) шарошечными долотами предложена трехмерная модель, решение которой осуществляется с применением численного объединенного метода гидродинамики сглаженных частиц и конечных элементов. На основе расчетов приведены оптимальные характеристики процесса разрушения горной породы с использованием указанных долот.

**Hamar hissələrin hidrodinamikası – son elementlərin birləşdirilmiş
üsulu əsasında polikristalitik almaz kompakt qazıma baltası vasitəsilə
süxurların dağıdılması prosesinin ədədi modelləşdirilməsi**

J.Pey, Z.Yinqhu, V.Jenquan, S.Donqyu
(Çin Neft Universiteti)

Xülasə

Polikristallik kompakt almaz (PKA) şaroşkalı qazıma baltaları ilə süxurların dağıdılması prosesində əsas dinamik xüsusiyyətlərin öyrənilməsi məqsədilə üç ölçülü model təklif edilir ki, bunun da həlli hamar hissələrin hidrodinamikası və son elementlərin birləşdirilmiş üsulunun tətbiqi ilə həyata keçirilir. Hesablamaların əsasında adıçəkilən baltaların istifadəsi ilə dağ süxurlarının dağıdılması prosesinin optimal xüsusiyyətləri verilir.